Cerebral Cortex, June 2017;27: 3294–3306

doi: 10.1093/cercor/bhx076
Advance Access Publication Date: 5 April 2017
Original Article

ORIGINAL ARTICLE

Intrinsic Connectivity Network-Based Classification and Detection of Psychotic Symptoms in Youth With 22q11.2 Deletions

Matthew Schreiner[1,2,†], Jennifer K. Forsyth[3,†], Katherine H. Karlsgodt[3], Ariana E. Anderson[1], Nurit Hirsh[3], Leila Kushan[3], Lucina Q. Uddin[4,5], Leah Mattiacio[6], Ioana L. Coman[6], Wendy R. Kates[6] and Carrie E. Bearden[1,3]

[1]Department of Psychiatry & Biobehavioral Sciences, University of California, Los Angeles, CA 90095, USA, [2]Interdepartmental Neuroscience Program, University of California, Los Angeles, CA 90095, USA, [3]Department of Psychology, University of California, Los Angeles, CA 90095, USA, [4]Department of Psychology, University of Miami, Coral Gables, FL 33124, USA, [5]Neuroscience Program, University of Miami Miller School of Medicine, Miami, FL 33136, USA and [6]Department of Psychiatry and Behavioral Sciences, SUNY Upstate Medical University, New York, NY 13210, USA

Address correspondence to Carrie E. Bearden, A7-460 Semel Institute, Los Angeles, CA 90095, USA. E-mail: cbearden@mednet.ucla.edu

[†]Co-first author.

Abstract

22q11.2 Deletion syndrome (22q11DS) is a genetic disorder associated with numerous phenotypic consequences and is one of the greatest known risk factors for psychosis. We investigated intrinsic-connectivity-networks (ICNs) as potential biomarkers for patient and psychosis-risk status in 2 independent cohorts, UCLA (33 22q11DS-participants, 33 demographically matched controls), and Syracuse (28 22q11DS, 28 controls). After assessing group connectivity differences, ICNs from the UCLA cohort were used to train classifiers to distinguish cases from controls, and to predict psychosis risk status within 22q11DS; classifiers were subsequently tested on the Syracuse cohort. In both cohorts we observed significant hypoconnectivity in 22q11DS relative to controls within anterior cingulate (ACC)/precuneus, executive, default mode (DMN), posterior DMN, and salience networks. Of 12 ICN-derived classifiers tested in the Syracuse replication-cohort, the ACC/precuneus, DMN, and posterior DMN classifiers accurately distinguished between 22q11DS and controls. Within 22q11DS subjects, connectivity alterations within 4 networks predicted psychosis risk status for a given individual in both cohorts: the ACC/precuneus, DMN, left executive, and salience networks. Widespread within-network-hypoconnectivity in large-scale networks implicated in higher-order cognition may be a defining characteristic of 22q11DS during adolescence and early adulthood; furthermore, loss of coherence within these networks may be a valuable biomarker for individual prediction of psychosis-risk in 22q11DS.

Key words: intrinsic connectivity networks, machine learning, psychosis, resting state functional MRI, velocardiofacial syndrome

Introduction

22q11.2 Deletion syndrome (Velocardiofacial/DiGeorge syndrome; OMIM #192430; 22q11DS) is a genetic disorder affecting 1 in 2000–4000 live births, which results from a variable length hemizygous deletion (comprising some 30–60 genes) on chromosome 22 (Shaikh et al. 2000; Drew et al. 2011). While the deletion confers a wide range of phenotypic consequences, including palate anomalies, cardiac defects, dysmorphic facial features, immune deficiencies, and hypocalcemia, it is most notable for the cognitive dysfunction and heightened risk of developmental neuropsychiatric disease (particularly psychotic spectrum disorder) it imparts (Murphy 2002; Monks et al. 2014; Schneider et al. 2014). Accordingly, 22q11DS offers a unique opportunity to examine early neural biomarkers relevant to the development of psychosis in a genetically vulnerable population (Debbane et al. 2012; Schreiner et al. 2013; Meechan et al. 2015).

Resting state functional MRI (rs-fMRI) holds promise as a method for uncovering a neural signature that may serve as such a biomarker. Since the first reports of correlations in spontaneous brain activity across spatially distinct areas of the cortex, the analysis of rs-fMRI data has rapidly grown to become an established field in its own right (Biswal et al. 1995; Van Den Heuvel and Hulshoff 2010). Leveraging these approaches, a large number of studies have now documented disrupted intrinsic functional architecture in individuals suffering from idiopathic psychotic illness, and have shown associations between intrinsic functional connectivity and behavioral outcomes (Broyd et al. 2009; Anticevic et al. 2014; Littow et al. 2015). Simultaneously, the emergence of machine learning approaches to neuroimaging data has increasingly demonstrated great promise for identifying predictors of unexplained variance in outcomes (Uddin et al. 2013; Plitt et al. 2015). Recent work in 22q11DS has characterized alterations in intrinsic connectivity networks (ICNs) and the behavioral correlates of these aberrations via a range of analysis methods, from classic hypothesis-driven region-of-interest or seed-based approaches to data-driven independent component analysis (ICA) and graph theoretical approaches. Our group's initial examination of functional connectivity in 22q11DS used an a priori, seed-based approach to uncover evidence of weakened long-range connectivity between the posterior cingulate and ventromedial prefrontal cortex, the 2 major hubs of the default mode network (DMN), and an association between the strength of this long-range connectivity and social behavior (Schreiner et al. 2014). The first published study to investigate multiple resting state networks in 22q11DS utilized dimension-restricted ICA to identify both increased and decreased functional connectivity within several ICNs (including the DMN), and showed a relationship between prodromal symptom severity and DMN strength (Debbane et al. 2012). More recently, this same group applied a support vector machine (SVM) classifier to graph theory connectivity matrices to distinguish between 22q11DS subjects and controls, showing that the strength of functional connections largely within the frontal lobe offered the strongest predictor of group membership (Scariati et al. 2014). However, these findings were not validated in an independent cohort, and previous research has shown that regularized logistic models that encourage sparsity provide a more robust and accurate prediction of diagnostic status than can be achieved within an SVM-framework (Ryali et al. 2010). Despite the important groundwork laid by these initial forays, the small sample sizes, and wide variation in image processing streams and methodologies across studies highlights the need for robust, reliable biomarkers that can be independently validated. Here we investigated the complete range of ICNs in individuals with 22q11.2 deletions and typically developing controls using an unbiased, data-driven approach (Beckmann and Smith 2004). The goal of these analyses was to: (1) identify measures of within-network connectivity that could accurately distinguish participants with 22q11DS from typically developing controls and (2) predict psychosis risk status on an individual basis. Based on prior findings in other neurodevelopmental disorders indicating disruption of resting networks that predicted both case-control status (Uddin et al. 2013) and behavioral outcomes (Plitt et al., 2015), we predicted that alterations in large scale networks involved in higher-order and social cognition (i.e., default mode, executive, and salience networks) may discriminate 22q11DS patients from controls, and be related to psychosis risk status.

Materials and Methods

Participants

The initial sample, consisting of 66 participants aged 8–20 years (33 patients with a molecularly confirmed diagnosis of a 22q11.2 microdeletion and 33 age- and sex-matched typically developing controls), was recruited from an ongoing longitudinal study at the University of California, Los Angeles. Exclusion criteria for all study participants were additional neurological or medical condition that might affect neuroimaging measures, insufficient fluency in English, substance or alcohol abuse and/or dependence within the past 6 months, and/or any condition that is a contraindication for MRI (pregnancy, claustrophobia, etc.). Healthy controls additionally did not meet criteria for any major mental disorder, based on information gathered during administration of the Structured Clinical Interview for DSM-IV Axis I Disorders (SCID) (First et al. 1996), with an additional developmental disorders module, as applied by Addington et al. (2012), for participants over the age of 16 years, and/or the Computerized Diagnostic Interview Schedule for Children (C-DISC) (Shaffer et al. 1996) for participants aged ≤16 years. Healthy controls additionally could not meet criteria for a prodromal state, as assessed by the Structured Interview for Prodromal Syndromes (SIPS) (Miller et al. 2003). All clinical interviews were conducted by highly trained MA- or PhD-level psychologists; inter-rater reliability and case consensus procedures have been described in detail elsewhere (Ho et al. 2012; Jalbrzikowski et al. 2012). All participants and/or their parents underwent a verbal and written informed consent process after complete description of the study. The UCLA Institutional Review Board approved all study protocols and all participants provided informed consent.

The unique replication dataset consisted of 56 participants ages 18–26 (28 patients with a molecularly confirmed diagnosis of a 22q11.2 microdeletion and 28 age- and sex-matched typically developing controls) ascertained at SUNY Upstate Medical University in Syracuse, NY, from an ongoing longitudinal study. Exclusion criteria matched that described above. The SUNY Institutional Review Board approved all study protocols and all participants provided informed consent.

Table 1 provides demographic information for all participants included in our analyses, following exclusion of subjects with excess motion (see below) during their scan. There were no participants who were previously on antipsychotics, but no longer taking antipsychotics. Demographics of UCLA and

Table 1 Subject demographics for UCLA and Syracuse cohorts

	22q11DS	Control	P-value
UCLA cohort			
N	33	33	–
Mean age ± SD [range]	14.03 ± 3.75 [8–20]	13.61 ± 3.44 [8–20]	0.63
% Male	42	52	0.47
Mean motion (mm), mean ± SD	0.14 ± 0.13	0.11 ± 0.09	0.25
SIPS score, mean ± SD	5.2 ± 5.6	1.2 ± 1.5	0.0007
Full scale IQ , mean ± SD	79.8 ± 14.6	106.9 ± 19.2	<0.0001
N_{ADHD}	15	2	<0.0001
N_{ASD}	17	0	<0.0001
Medication status	7 Antidep, 2 antipsy	1 Antidep	0.02
Scanner site	BMC: 15, CCN: 18	BMC: 17 CCN: 16	0.63
Syracuse cohort			
N	28	28	–
Mean age ± SD [range]	21.29 ± 2.46 [18–26]	20.79 ± 1.52 [18–26]	0.37
% Male	60.7	53.6	0.60
Mean motion (mm), mean ± SD	0.09 ± 0.04	0.08 ± 0.03	0.24
SIPS score, mean ± SD	2.7 ± 4.9	0.3 ± 1.2	0.01
N_{ADHD}	5	4	0.72
N_{ASD}	4	0	0.04
Full scale IQ, mean ± SD	76.6 ± 13.1	108.2 ± 15.8	<0.0001
Medication status	5 Antidep, 3 antipsy	2 Antidepressant	0.08

SIPS score = total positive symptom severity, Structured Interview for Prodromal Syndromes; N_{ADHD} = number of subjects with diagnosis of Attention Deficit Hyperactivity Disorder; N_{ASD} = Number of subjects with Autism Spectrum Disorder; antidep = antidepressant; antipsy = antipsychotic; BMC = brain mapping center; CCN = Center for Cognitive Neuroscience.

Syracuse cohorts were similar, except the Syracuse subjects were significantly older than the subjects in the UCLA sample ($P < 0.0001$). There were no significant differences between the UCLA and Syracuse cohorts in patient characteristics (i.e., SIPS score, IQ, or medication status). A previous publication included 71% (47/66) of the participants in the current UCLA cohort, in which an a priori seed-based approach was utilized to characterize rs-fMRI connectivity specifically within the DMN (Schreiner et al. 2013). Previous publications have reported on neurocognitive, anatomical, and clinical findings in the participants in the Syracuse cohort (Antshel et al. 2010; Coman et al. 2010; Roizen et al. 2010; Kates et al. 2011; McCarthy et al. 2015), but did not include resting state fMRI data. A recent publication by our Syracuse collaborators (Mattiaccio et al. 2016) reports on the association between resting-state network connectivity and clinical symptoms measured by the Brief Psychiatric Rating Scale, verbal memory, and executive functioning, in a partially overlapping sample.

Neurobehavioral Measures

All subjects from the UCLA sample over age 10 ($N = 56$; 28 22q11DS, 28 controls) were interviewed with the SIPS by a trained clinical interviewer, to assess the presence and severity of psychotic symptoms. 22q11DS individuals were categorically defined as being at high risk of conversion to psychosis based on the presence of any positive symptom rated in the prodromal or psychotic range, that is, a rating of 3 or higher on any item in the positive symptom subscale of the SIPS ($22q_{HR}$, $N = 10$). Low Risk was defined as having no positive symptoms in the prodromal /psychotic range ($22q_{LR}$, $N = 18$). The SIPS interview was also applied to all subjects in the Syracuse sample ($N = 56$, 28 22q11DS, 28 controls), and 22q11DS subjects were again divided into high risk ($22q_{HR}$, $N = 8$) and low risk ($22q_{LR}$, $N = 20$) groups. The $22q_{HR}$ and $22q_{LR}$ groups did not differ in demographic characteristics (e.g., age, gender, IQ, or scanner site) within either cohort (Supplementary Table 1).

MRI Acquisition

UCLA

Structural and functional scans for the UCLA sample were acquired at either the Ahmanson–Lovelace Brain Mapping Center (BMC) or the Staglin Center for Cognitive Neuroscience (CCN) in Los Angeles, CA, USA. Both sites had an identical 3 T Siemens Tim Trio system, utilizing a 12-channel head coil. 22q11DS subjects and control subjects were split equally between the 2 scanner sites, the scanning protocols implemented at each site were identical and analysis of potential between-scanner differences revealed no regions of differential cortical activation between scanner locations. The primary structural scan used for registration purposes consisted of a matched-bandwidth high resolution T1 image (voxel size 1.5 × 1.5 × 4.0 mm^3, echo time [TE] = 34 ms, repetition time [TR] = 5000 ms, echo spacing = 0.89 ms, 34 axial slices, slice thickness 4.0 mm, slice spacing 0 mm, flip angle 90°, field of view [FOV] = 210, matrix size = 128 × 128). Subsequently, a 5-min resting state functional scan was acquired, during which a black screen was presented and participants were instructed to keep their eyes open, remain relaxed, and attempt to avoid falling asleep. The resting state scan consisted of 152 BOLD 3D images (voxel size 3.0 × 3.0 × 4.0 mm^3, TE = 30 ms, TR = 2000 ms, echo spacing = 0.79 ms, 34 axial slices, slice thickness 4.0 mm, slice spacing 0 mm, flip angle 90°, FOV = 192, matrix size = 64 × 64).

SUNY Upstate (Syracuse)

Structural and functional scans for the Syracuse sample were acquired at SUNY Upstate Medical University, Syracuse, NY, USA. The scan site utilized a 3 Tesla Siemens Tim Trio system, with an 8-channel head coil. The primary structural scan used

for registration purposes consisted of a matched-bandwidth high resolution T1 image (voxel size 1.0 × 1.0 × 1.0 mm^3, TE = 3.31 ms, TR = 2530 ms, echo spacing = 7.6 ms, 176 axial slices, slice thickness 1.0 mm, slice spacing 7 mm, flip angle 7°, FOV = 256, matrix size = 256 × 256). Subsequently, a 5-min resting state functional scan was acquired, during which a black screen was presented and participants were instructed to keep their eyes open, remain relaxed, and attempt to avoid falling asleep. The resting state scan consisted of 152 BOLD 3D images (voxel size 4.0 × 4.0 × 4.0 mm^3, TE = 30 ms, TR = 2000 ms, echo spacing = 0.79 ms, 34 axial slices, slice thickness 4.0 mm, slice spacing 0 mm, flip angle 90°, FOV = 192, matrix size = 64 × 64).

Data Preprocessing

All data (from both the UCLA and Syracuse cohorts) were preprocessed and analyzed blind to diagnostic status with tools from the FMRIB Software Library (FSL; fsl.fmrib.ox.ac.uk/fsl) using standard practices (Supplementary Information). Each subject's full functional scan was motion-corrected by registering each image to the middle volume as a reference, using FMRIB's linear image registration tool. Any subject with >3 mm of translational motion or >3° of rotational motion was excluded from further analysis. This resulted in the exclusion of two 22q11DS patients and 2 control subjects at UCLA, and one 22q11DS subject at Syracuse, from the larger pool of subjects at each site from which the demographically matched 22q11DS patients and controls included in the study were selected. Accordingly, no subject in the final N = 66 UCLA cohort or N = 56 Syracuse cohort was discarded due to excess motion. Further characterization of motion was conducted using root mean square (RMS) volume-to-volume displacement of each brain volume relative to the previous volume (i.e., relative displacement; Jenkinson et al., 2002). Mean RMS motion is provided in Table 1. Additional indices of motion are provided in Supplementary Table 2; there were no significant differences between the patient and control groups in any motion indices at UCLA or Syracuse.

Group ICA, Network Identification, and Dual Regression

Following initial preprocessing, the individual fMRI scans were entered into FSL's MELODIC toolbox, for single-session ICA (ssICA), as in Kelly et al. 2010, and Griffanti et al. 2014. ssICA decomposed each individual's 4D scan into a series of different spatial and temporal components, some of which represented underlying ICNs and some of which represented artifacts related to motion, scanner drift and/or extraneous physiological noise. De-noised fMRI scans (Supplementary Information for details) were then concatenated across all subjects in the UCLA cohort and entered into a group ICA (gICA) session (Calhoun et al. 2009). Brain Nexus templates (Thomason et al., 2011; www.brainnexus.com/resources/resting-state-fmri-templates) were used to identify plausible ICNs and a Dual Regression approach was used to generate subject-specific versions of the relevant gICA components (Beckmann 2009). Each ICN was tested for group differences in both directions; significant clusters were identified using threshold-free cluster enhancement with family-wise-error correction (Supplementary Information for details).

Network-Derived Classifiers

For each of the 66 participants from the UCLA cohort, subject-specific spatial maps for each of 12 ICNs (reported below) were restricted to a thresholded ($Z > 4.3$; $P < 0.0001$) mask of the group-average ICN from the gICA. These thresholded maps were vectorized and entered into a regularized logistic regression classifier, to analyze the ability of classifiers derived from each ICN to accurately distinguish between patients and controls. The classification algorithm used was lassoglm (www.mathworks.com/help/stats/lassoglm.html), a tool bundled with the Statistics Toolbox for MATLAB that utilizes L1-regularization to impose a sparse weight selection to predictors such that most features have zero weight. This algorithm was implemented to mitigate the potential for over-fitting given the large number of predictors (i.e., voxels) for each ICN relative to observations (i.e., subjects). Leave-one-out cross-validation (LOOCV) optimized the regularization parameter to generate final models of in-network voxels for each ICN that would both robustly predict group membership in the training dataset and be likely to generalize to independent datasets (Tibshirani 1996; Ng 2004; Uddin et al. 2013). The final models were applied back to the UCLA sample to examine training error within the UCLA cohort, and then tested/validated in the independent Syracuse dataset, as described below. We report number of subjects misclassified, accuracy, sensitivity, and specificity for each ICN-based classifier. Inference was accomplished by computing a bootstrap distribution of null classifier models, to aid in calculation of P-values that assess significance of a given ICN's classification accuracy.

A nested cross-validation procedure was additionally implemented for each ICN within the training set to generate performance estimates of UCLA-trained classifiers as applied to independent samples (Varoquax et al. 2017). Thus, 2 LOOCV loops were run, one inside the other; the inner cross-validation loop was used to set the optimal regularization parameter, while the external loop varying the left out fold was used to calculate average accuracy using the left out sample (i.e., to generate estimates of model accuracy in new data not used for model parameter estimation). Cross-validated estimates of number of subjects misclassified and classification accuracy are provided.

Classifier-Based Prediction of Psychosis Risk Status

To examine potential relationships between within-network connectivity and psychotic symptom severity in the 22q11DS group, we trained a variation of the lassoglm algorithm described above on the subset of UCLA-22q11DS subjects with SIPS data (N = 28, ages 10–20 years), in order to determine the ability of voxels within a particular ICN to accurately partition these subjects into high risk (HR) ($22q_{HR}$) or low risk (LR) ($22q_{LR}$) categories on the basis of their within-network connectivity (Supplementary Information). The final models were similarly applied back to the UCLA sample to examine training error, and tested in the independent Syracuse dataset. A nested cross-validation procedure was additionally implemented to generate performance estimates of UCLA-trained classifiers as applied to independent samples.

Validation of Classifiers in Syracuse Dataset

For each ICN, the UCLA-trained diagnostic classifier was applied to the subjects from the Syracuse cohort, to test the generalizability of each classifier for distinguishing between 22q11DS patients and controls in this independent cohort of young adults (N = 56) (Pereira et al. 2009). P-values for the logistic-regression diagnostic classifiers were calculated from a

bootstrap distribution of null models and are Bonferroni-corrected, for all networks tested.

Logistic regression classifiers trained to assess prodromal risk status in the UCLA sample were similarly applied to the Syracuse testing dataset, to obtain a measure of their ability to generalize to a unique sample of 22q11DS subjects ($N = 28$).

Results

Group Differences in Functional Connectivity

gICA on the UCLA sample of $N = 66$ subjects yielded 32 independent components when utilizing ADE to extract the optimal number of components to describe the data. From these 32 components, the template-matching procedure identified 12 putative ICNs of interest: DMN, posterior DMN, anterior cingulate (ACC)/precuneus network, a merged auditory/middle temporal network (AUD/TEMP), visual network, motor network, supplementary motor network (SUPP MOT), left (LEFT EXEC) and right (RIGHT EXEC) lateralized executive networks, combined executive network (COMB. EXEC), parietal association network (PAR ASSOC) and salience network (SAL) (Fig. 1). For 22q11DS patients versus controls, no significant ICN hyperconnectivity survived the multiple comparison correction and stringent FWE-rate criteria applied by randomize, but significantly reduced functional connectivity (i.e., within-ICN hypoconnectivity) was observed in 5 of the 12 networks: ACC/precuneus network, DMN, posterior DMN, combined executive, and salience networks (Fig. 2). Within the ACC/Precuneus network, significantly weaker functional connectivity in 22q11DS subjects was localized to the paracingulate gyrus, medial prefrontal cortex (mPFC), superior frontal gyrus and vmPFC. Location, size, and significance of clusters surviving multiple comparison correction are reported in Table 2A.

Single-subject de-noising, gICA, ICN identification, and dual regression were performed on the Syracuse cohort in an identical manner to the procedures described above for the UCLA data. Among the ICNs identified using gICA and template matching in the Syracuse cohort (Supplementary Figure 1), a highly similar pattern of 22q11DS within-network hypoconnectivity was found in 5 ICNs (Table 2B). Specifically, clusters of within-network hypoconnectivity were observed in predominantly frontal and posteromedial cortical regions, in the left and right executive network, DMN, posterior DMN, and a combined ACC/precuneus and salience network. Clusters showing significant within-ICN hypoconnectivity across both the UCLA and Syracuse cohorts is shown in Supplementary Figure 2.

22Q11DS Versus Control Classifier Performance in Training Dataset

The accuracy of the classifiers derived from each ICN as applied to the UCLA training set are shown in Table 3, along with cross-validated estimates for the performance of each classifier for independent cohorts. Of the 12 ICNs defined above in the training set, 10 classifiers were able to correctly discriminate between 22q11DS patients and controls at a greater than chance (50%) level in the UCLA cohort, on the basis of within-network connectivity alone (Fig. 3). The average classification accuracy was 87% across all ICN-derived classifiers (including those trained on connectivity from within the Right Executive network and Motor Network, the 2 classifiers which did not perform above chance).

22Q11DS Versus CONTROL Classifier Testing in Syracuse Cohort

Following training of the ICN-derived classifiers on the UCLA cohort, the 22Q11DS versus Control classifiers were applied to the Syracuse cohort ($N = 56$) for testing/validation (Fig. 3). Of the 12 ICN-derived classifiers examined, 3 maintained significant accuracy ($P < 0.0042$) when applied to this unique sample, despite the noted age difference between cohorts. The ACC/precuneus network-derived classifier correctly identified 21 of 28 patients with 22q11DS (75% sensitivity) and 20 of 28 controls (71% specificity) in the Syracuse cohort, achieving a classification accuracy of 73.2% overall ($P = 0.0033$). The DMN-derived classifier correctly identified 27 of 28 patients with 22q11DS (96% sensitivity) and 13 of 28 controls (46% specificity), achieving a classification accuracy of 71.4% overall ($P = 0.0029$). The posterior DMN-derived classifier correctly identified 24 of 28 patients with 22q11DS (86% sensitivity) and 18 of 28 controls (64% specificity), achieving a classification accuracy of 75% overall ($P = 0.0011$). Full results on the performance of the ICN-derived classifiers in the testing (Syracuse) dataset are also presented in Table 3.

Classifier Prediction of Psychosis Risk Status in the UCLA dataset

For each ICN, sparse linear regression (i.e., the Lasso) was able to generate a compact model of within-network voxels that robustly predicted positive prodromal symptom severity in UCLA-22q11DS patients. Using the voxels identified by the Lasso, a logistic regression model was fit to optimally discriminate between $22q_{HR}$ and $22q_{LR}$ subjects within the UCLA cohort ($N_{HR} = 10$, $N_{LR} = 18$) (Fig. 4). The average training accuracy was 82% across all ICN-derived classifiers. For each classifier, we report the total subjects misclassified, overall accuracy, sensitivity, and specificity within UCLA (i.e., training error), as well as the nested cross-validated estimates of number of subjects misclassified and average accuracy in Table 4.

$22Q_{HR}$ Versus $22Q_{LR}$ Classifier Testing With Syracuse Dataset

Following training of the ICN-derived classifiers on the 22q11DS subjects from the UCLA cohort, the HR versus LR classifiers were applied to the 22q11DS subjects from the Syracuse cohort ($N_{HR} = 8$, $N_{LR} = 20$) for testing/validation (Fig. 4 and Table 4). Across the 12 ICN-derived classifiers, average classification accuracy was 78%. Four of the 12 ICNs maintained significant accuracy ($P < 0.0042$) when applied to the unique testing cohort: specifically, classifiers derived from the ACC/precuneus network (86% overall classification accuracy; $P = 0.0002$), DMN (82%; $P = 0.0004$), left executive network (79%; $P = 0.0019$), and salience network (79%; $P < 0.0001$).

Robustness of Group Differences and Classifier Performance to Motion

Motion was similar between 22q11DS and control subjects (Supplementary Table 2) and between $22q_{HR}$ and $22q_{LR}$ subjects for both cohorts (Supplementary Table 1). Given that similar patterns of hypoconnectivity were seen in 22q11DS subjects relative to controls when analyses were restricted to subjects with minimal motion, it is highly unlikely that differences in

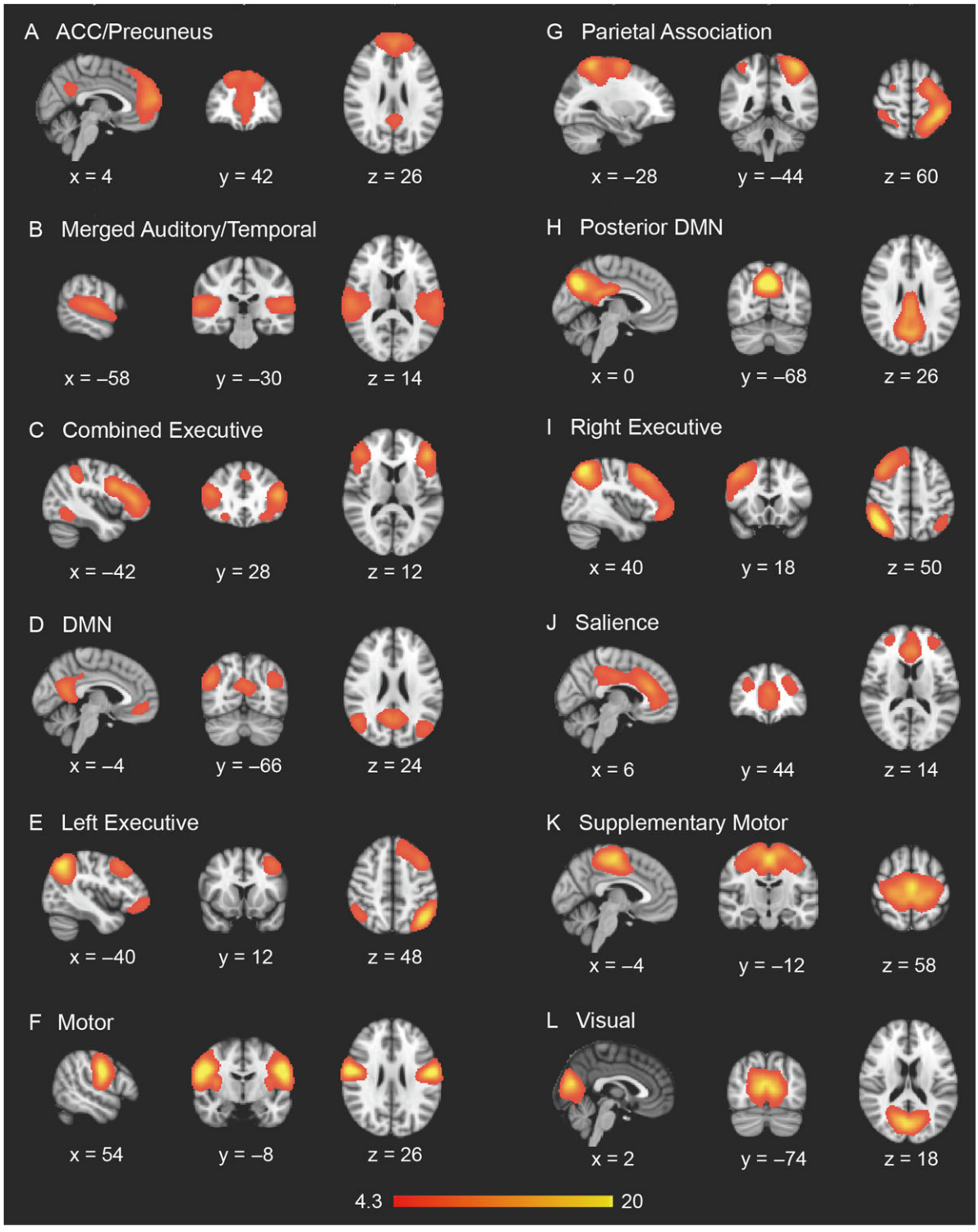

Figure 1. Intrinsic connectivity networks identified via gICA (implemented with automatic dimensionality estimation) in the UCLA sample.

motion account for group differences in connectivity across these ICNs (Supplementary Information Section 1.7 for details). Additionally, the accuracy of the ICN-derived classifiers that significantly distinguished between 22q11DS and control subjects and between $22q_{HR}$ and $22q_{LR}$ across sites was similar in subgroups of subjects with minimal motion (Supplementary Tables 11–14).

Sensitivity Analyses

As Attention Deficit Hyperactivity Disorder (ADHD) and Autism Spectrum Disorder (ASD) are common comorbidities for those diagnosed with 22q11DS, we sought to determine whether the ICN-derived classifiers trained to differentiate between HR and LR subjects could also detect the presence of ADHD (N = 11) or

ASD (*N* = 14) in the 22q11DS subjects in our data. These follow-up analyses revealed that none of the ICN-derived HR versus LR classifiers were able to accurately distinguish between 22q11DS subjects with ADHD and those without an ADHD diagnosis, nor those with or without an ASD diagnosis, in the training and testing cohorts.

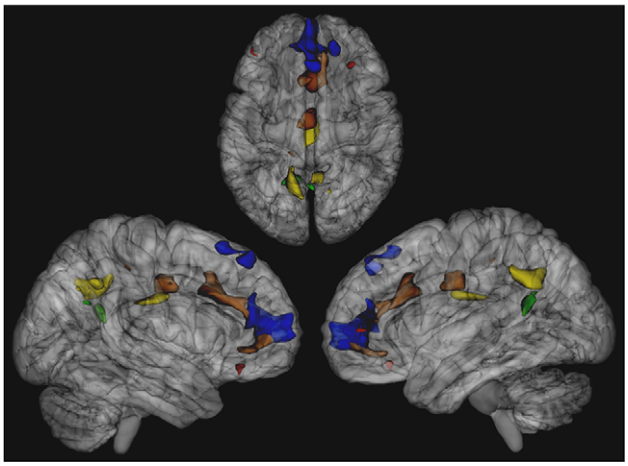

Figure 2. Cluster locations of significant 22q11DS within-ICN hypoconnectivity for various networks, derived from the UCLA cohort. ACC/Precuneus Network rendered in blue, combined executive network rendered in red, DMN rendered in green, posterior DMN rendered in yellow, salience network rendered in brown.

Discussion

This study is the first to investigate multiple ICNs in 2 independent samples of patients with 22q11.2 deletions and demographically comparable typically developing controls. Several novel findings emerged, in particular: (1) consistent and replicable patterns of hypoconnectivity exist within large-scale brain networks implicated in higher order cognition in 22q11DS during adolescence; (2) hypoconnectivity signatures in the ACC/precuneus, DMN, and posterior DMN could reliably distinguish individuals with 22q11DS from controls in an independent sample; and (3) hypoconnectivity in the ACC/precuneus, DMN, left executive, and salience networks reliably differentiated between 22q11DS subjects at high and low risk for psychosis in 2 independent cohorts.

Our findings of within-network hypoconnectivity in 22q11DS across several ICNs are largely consistent with established literature in 22q11DS and idiopathic schizophrenia (Broyd et al. 2009; Scariati et al. 2014). Indeed, significantly reduced functional connectivity in patients with idiopathic schizophrenia relative to matched controls has previously been observed within the posterior cingulate and precuneus

Table 2 (A) Clusters of significant ICN-hypoconnectivity in the UCLA cohort. (B) Clusters of significant ICN-hypoconnectivity in the Syracuse cohort

Network	Cluster index	Voxels	*P*-value	MNI coords			MNI Location
				X	Y	Z	
(A) UCLA							
ACC/precuneus	4	933	<0.001	−2	48	−4	Paracingulate gyrus
	3	213	0.001	4	26	52	Superior frontal gyrus
	2	147	0.001	18	42	44	Right frontal pole
	1	1	0.002	2	48	−12	mPFC
Comb. executive	2	50	0.001	32	32	−12	Right OFC
	1	28	0.002	−46	44	2	Left frontal pole
DMN	2	185	<0.001	−16	−56	18	Left precuneus
	1	1	0.002	18	−54	24	Right precuneus
Posterior DMN	4	316	<0.001	−14	−56	28	Left precuneus
	3	226	<0.001	2	−16	30	PCC
	2	119	<0.001	6	−52	38	Right precuneus
	1	18	0.002	14	−62	34	Right precuneus
Salience	5	573	<0.001	4	16	28	ACC
	4	402	<0.001	0	50	−4	Paracingulate gyrus
	3	276	0.001	−2	−12	30	ACC, PCC
	2	19	0.002	−12	−36	46	Pre/postcentral gyrus
	1	3	0.002	−32	18	−12	Left OFC
(B) Syracuse							
ACC/PRECUN + SAL	2	1715	<0.001	−2	52	−6	mPFC,ACC
	1	95	0.001	−24	52	16	Left frontal pole
DMN	2	154	<0.001	−4	−50	16	PCC
	1	54	0.001	18	−52	18	Precuneus
Posterior DMN	2	243	<0.001	0	−34	22	PCC
	1	4	0.001	−44	−64	52	Left dlOCC
Right executive	2	247	<0.001	44	−54	48	Angular gyrus, right SPL
	1	53	0.001	42	50	10	Right frontal pole
Left executive	2	48	<0.001	−42	−64	52	Left dlOCC
	1	27	0.001	−18	56	22	Left frontal pole

mPFC = medial prefrontal cortex; OFC = orbitofrontal cortex; PCC = posterior cingulate cortex; ACC = anterior cingulate cortex; ACC/PRECUN + SAL = merged ACC/precuneus and salience network; dlOCC = dorsolateral occipital cortex; SPL = superior parietal lobule.

Table 3 Performance of ICN-derived classifiers at distinguishing between 22q11DS subjects and controls within training (UCLA) and testing (Syracuse) cohorts

Network	Training set (UCLA)							Testing set (Syracuse)				
	Training performance					Cross-validated estimates						
	MIS	% AC	SENS	SPEC	P	MIS	% AC	MIS	% AC	SENS	SPEC	P
ACC/PRECUN	2	97	1	0.94	<0.001	12	82	15	73	0.75	0.71	0.003
AUD/IFG	3	95	0.97	0.94	<0.001	20	70	20	64	0.82	0.46	0.077
COMB EXEC	3	95	0.97	0.94	<0.001	17	74	23	59	0.57	0.61	0.531
DMN	0	100	1	1	<0.001	6	91	16	71	0.96	0.46	0.003
LEFT EXEC	1	98	1	0.97	<0.001	20	70	16	71	0.79	0.64	0.007
Motor	33	50	1	0	1	66	0	28	50	1	0	0.999
PAR ASSOC	1	98	1	0.97	<0.001	18	73	18	68	0.71	0.64	0.03
Post DMN	5	92	0.97	0.88	<0.001	18	73	14	75	0.86	0.64	0.001
RIGHT EXEC	33	50	1	0	1	65	2	28	50	1	0	0.999
Salience	2	97	1	0.94	<0.001	22	67	20	64	0.57	0.71	0.088
SUPP MOT	11	83	0.88	0.79	<0.001	37	44	24	57	0.57	0.57	0.61
Visual	11	83	0.94	0.73	<0.001	24	64	22	60	0.86	0.29	0.427

AUD/IFG = auditory cortex/inferior frontal gyrus network; COMB EXEC = combined executive network; PAR ASSOC = parietal association network; post DMN = posterior default mode network; SUPP MOT = supplementary motor network; MIS = subjects misclassified; % AC = percent accuracy; SENS = sensitivity; SPEC = specificity; PPV = positive predictive value; NPV = negative predictive value; P = P-value.

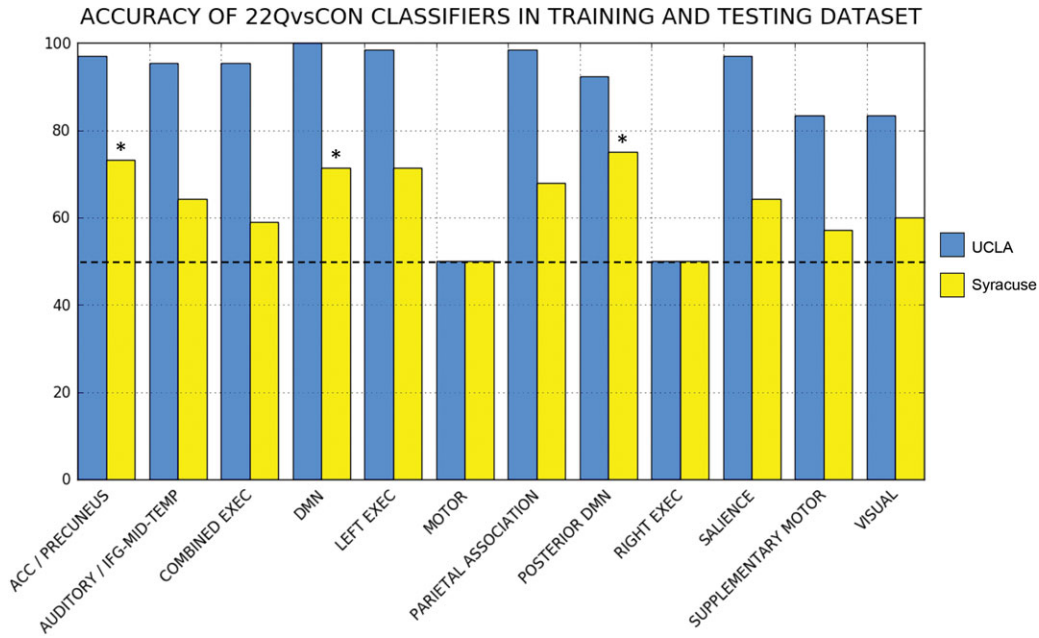

Figure 3. Classification accuracy of ICN-based diagnostic classifiers. The training cohort (UCLA) is shown in blue, and the replication cohort (Syracuse) is shown in yellow. Classifiers whose performance in the training and testing datasets remained significant after multiple comparison correction ($P < 0.0042$) are denoted with an asterisk.

(Calhoun et al. 2012); the same regions in which we observed localized clusters of ACC/precuneus and DMN hypoconnectivity in 22q11DS. In addition, our results from the Syracuse replication dataset exhibit striking similarities to our primary findings from the UCLA cohort, supporting the notion of general ICN hypoconnectivity as a defining characteristic of 22q11DS during adolescence and early adulthood. The first report of ICN dysfunction in 22q11DS subjects utilizing an ICA approach with a pre-specified number of components (Debbane et al. 2012), showed within-network connectivity differences in both directions, with (predominantly adolescent) 22q11DS patients showing regions of relative hypoconnectivity in a high-level visual processing network and the DMN, but also clusters of *hyper*connectivity in lower-level networks (visuospatial processing and sensorimotor networks) and the DMN. Using different methods from ours in a partially overlapping young adult sample, our Syracuse collaborators observed 22q11DS hyperconnectivity in mostly lower-level ICNs (sub-clusters of the low-level visual processing network, Limbic/Temporal, DMN and visuospatial processing networks) and hypoconnectivity in 22q11DS

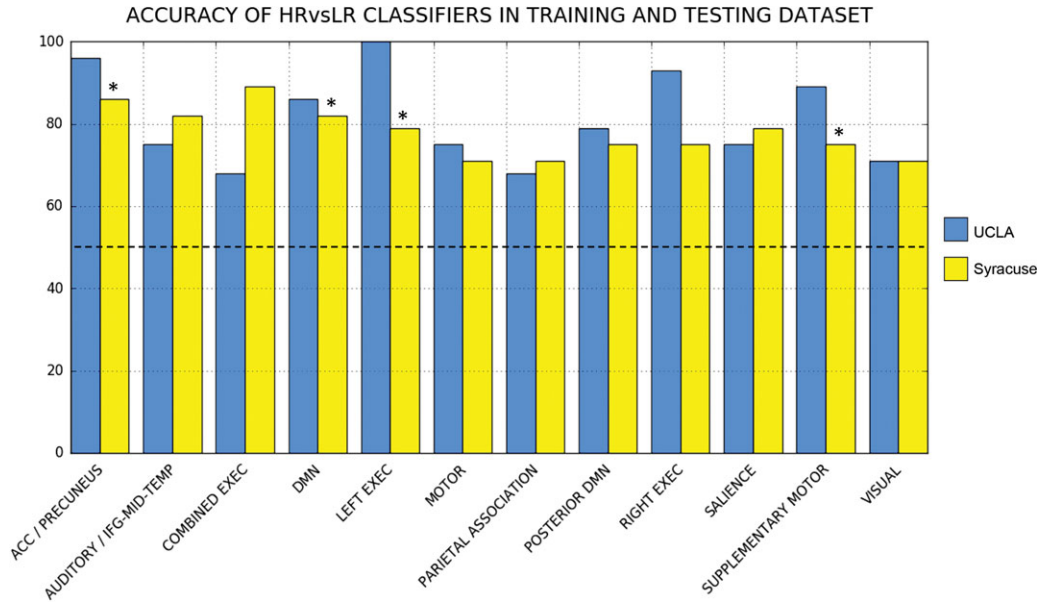

Figure 4. Classification accuracy of ICN-based classifiers for distinguishing 22q11DS patients at high (HR) versus low (LR) risk for psychosis. The training cohort (UCLA) is shown in blue, and the replication cohort (Syracuse) is shown in yellow. Classifiers whose performance in the training and testing datasets remained significant after multiple comparison correction ($P < 0.0042$) are denoted with an asterisk.

Table 4 Performance of ICN-derived classifiers at distinguishing between $22q_{HR}$ and $22q_{LR}$ subjects within training (UCLA) and testing (Syracuse) cohorts

Network	Training set (UCLA)							Testing set (Syracuse)				
	Training performance					Cross-validated estimates						
	MIS	% AC	SENS	SPEC	P	MIS	% AC	MIS	% AC	SENS	SPEC	P
ACC/PRECUN	1	96	1	0.94	<0.0001	1	96	4	86	0.75	0.9	0.0002
AUD/IFG	7	75	0.5	0.89	0.037	10	64	5	82	0.5	0.95	0.0006
COMB EXEC	9	68	0.4	0.83	0.041	5	82	3	89	0.88	0.9	<0.0001
DMN	4	86	0.8	0.89	0.0004	10	64	5	82	0.625	0.9	0.0004
LEFT EXEC	0	100	1	1	<0.0001	5	82	6	79	0.625	0.85	0.0019
Motor	7	75	0.4	0.94	0.042	10	64	8	71	0.125	0.95	0.0716
PAR ASSOC	9	68	0.2	0.94	0.284	7	75	8	71	0.125	0.95	0.0773
Post DMN	6	79	0.6	0.89	0.011	6	79	7	75	0.25	0.95	0.0166
RIGHT EXEC	2	93	0.9	0.94	<0.0001	1	96	7	75	0.25	0.95	0.0158
Salience	7	75	0.5	0.89	<0.0025	5	82	6	79	0.25	1	<0.0001
SUPP MOT	3	93	0.8	0.94	<0.0001	8	71	7	75	0.375	0.9	0.0155
Visual	8	71	0.3	0.94	0.012	6	79	8	71	0.125	0.95	0.0781

AUD/IFG = auditory cortex/inferior frontal gyrus network; COMB EXEC = combined executive network; PAR ASSOC = parietal association network; post DMN = posterior default mode network; SUPP MOT = supplementary motor network; MIS = subjects misclassified; % AC = percent accuracy; SENS = sensitivity; SPEC = specificity; P = P-value.

subjects largely within higher-order cognitive networks (e.g., precuneus, left and right executive and salience networks; Mattiaccio et al. 2016). In contrast, in our analyses, any findings of relative hyperconnectivity in 22q11DS patients—in both our adolescent UCLA cohort and the Syracuse young adult cohort—failed to survive correction for multiple comparisons. Despite these differences, the cluster locations of significant hypoconnectivity in 22q11DS patients reported by Debbane et al. (2012) and Mattiaccio et al. (2016) are consistent with those we report here; namely, in the precuneus, pre/postcentral gyrus, superior frontal gyrus, and medial frontal cortex. Accordingly, the numerous methodological differences in our processing streams and analysis choices could account for the discrepancies between studies.

Despite the age difference between the training and testing cohort, the ICN-derived classifiers trained on connectivity maps from the UCLA cohort were largely able to generalize to an independent cohort of older individuals, providing evidence for developmental stability of these connectivity deficits in 22q11DS. In particular, the pronounced alterations to long-

range functional connections anchored by the cingulate cortex, precuneus, and frontal cortex echo findings reported in the current literature on 22q11DS (Ottet et al. 2013). Moreover, the ability of ICN-derived classifiers to also accurately partition the training and testing 22q11DS cohorts into "High Risk" and "Low Risk" subgroups supports the notion that ICN hypoconnectivity in adolescence may be a relevant biomarker for psychosis risk (Broyd et al. 2009; Calhoun et al. 2012; Scariati et al. 2014; Alderson-Day et al. 2015; Alonso-Solís et al. 2015). The ICNs for which within-network connectivity was both robustly predictive of case-control status and HR versus LR status (within 22q11DS subjects) were the ACC/precuneus network and the DMN. These are both networks involving predominantly midline brain regions, suggesting functional disruption of these regions may be related to disrupted midline cortical development (Bearden et al. 2007).

Additionally, our findings are largely convergent with the wealth of studies in murine models of 22q11DS, indicating that the syndrome is a disorder of cortical circuit formation (Chun et al. 2014; Meechan et al. 2009, 2015); and further, that this neurodevelopmentally based hypoconnectivity has relevance for clinical symptomatology.

Applications of network-based diagnostic classifiers have become an area of intense research and interest in the neuroimaging community, and recent work has shown that regularized logistic regression approaches that encourage sparse models tend to outperform a SVM framework for classification problems involving fMRI data (Ryali et al. 2010; Mohr et al., 2015; Rosa et al. 2015). Our ability to achieve an average 22q11DS versus control classification accuracy of 96.3% within the training set when using sparse regularization to train classifiers derived from the ACC/precuneus, DMN, and posterior DMN ICNs, and to successfully apply these classifiers to a completely independent validation cohort with 73% accuracy is notable. Previous work utilizing a SVM-framework on graph theory based resting state connectivity matrices achieved a maximal cross-validation classification accuracy of 84% for distinguishing 22q11DS cases from controls in the training set, and did not test the performance of their classifier on any independent datasets (Scariati et al. 2014). Conversely, a classifier trained on the DMN in the present study showed a cross-validation accuracy estimate of 91% within the UCLA cohort, and achieved 71% accuracy in the independent cohort, despite the age difference between the 2 cohorts. Convergent with our current findings, previous research has consistently demonstrated that alterations in DMN extent and strength are associated with a range of cognitive deficits and psychotic symptoms, both in 22q11DS and idiopathic schizophrenia (Broyd et al. 2009; Debbane et al. 2012; Schreiner et al. 2013). Furthermore, the classifiers that yielded the most robust case-control classification accuracies in cross-validation and the testing set were largely derived from functional networks implicated in higher-order cognition (e.g., ACC/precuneus, DMN, posterior DMN, and executive networks), rather than those involved in basic sensory or motor processing. This parallels reports of the cognitive and behavioral deficits characteristic of the syndrome (Drew et al. 2011), and the central role these ICNs play in mediating cognitive processes (Menon 2011).

This overall case versus control classification is the first step in establishing algorithms that can distinguish those at HR for a psychiatric outcome (i.e., psychosis) from those at low risk. Notably, in the UCLA training cohort we also achieved a mean accuracy of 89.25% across the ACC/precuneus, DMN, left executive, and salience-derived classifiers for discriminating 22q11DS youth at high versus low risk for psychosis, with 81.5% accuracy in our testing/validation cohort. In the context of other genetic disorders (e.g., Huntington's disease), machine learning algorithms based on multivariate voxel patterns obtained from neuroimaging data have been shown to be valuable for generating quantitative measures predictive of disease progression that are strongly correlated with established measures of disease progression (Rizk-Jackson et al. 2011). Resting state functional connectivity data has also been shown to successfully predict heterogeneity in outcomes for individuals with ASD that could not be accounted for by behavioral indices (Plitt et al. 2015).

Few empirical studies have been published to date on ICNs in other neurogenetic syndromes. While findings are tentative due to small sample sizes, Vega et al. (2015) found reduced within-network connectivity in multiple ICNs in patients with Williams Syndrome versus typically developing controls. Similar to our 22q11DS population, youth with Williams Syndrome had markedly reduced within-network connectivity in the default mode and visual attention networks relative to controls. The authors suggest that altered brain morphology in William Syndrome, particularly in the corpus callosum, may influence interhemispheric connectivity; notably, similar anomalies of midline brain development are characteristic of 22q11DS (Bearden et al. 2007; Shashi et al. 2012). In contrast, patients with Down Syndrome had higher levels of between-network connectivity in several network pairs relative to controls, but no difference in within-network connectivity (Vega et al. 2015). These findings are consistent with a hypothesis of immature development of typical neural connectivity in Down Syndrome patients; clearly, more research on larger samples is needed, as well as translational studies in animal models, to better understand the neurobiological basis of the observed connectivity alterations across disorders.

Despite the overall convergence of results across the UCLA and Syracuse cohorts, we witnessed splitting and/or merging of some common ICNs in the Syracuse sample. Specifically, we observed that the components associated with the ACC/precuneus network, salience network, and parietal association network appeared to mix and overlap to some extent, and that a portion of the combined executive network appeared to merge with a portion of the right parietal association network. However, this apparent splitting/merging of the template-defined ICNs in the older cohort (aged 18–26 years) is to be expected, considering the maturation of resting state networks with age, and our decision to apply the same Brain Nexus templates (derived from subjects aged 9–15 years) for ICN-identification across samples for internal consistency and comparability. Importantly, the use of network templates available from the BrainMap database (derived from adults, age range 20–35 years), to identify components of interest in the UCLA and Syracuse cohort did not alter the ICNs identified, nor any of the subsequent results. With regard to the spatial overlap of several ICNs (e.g, the DMN and posterior DMN, or the ACC/precuneus and salience networks), we note that ICA does not extract components with spatial extents that are mutually exclusive of one another—rather, it attempts to maximize the spatial independence of the components, subject to the constraint that it minimize the unexplained variance in the raw data.

Despite our use of regularization to avoid over-fitting the classifier models to the input data, there are caveats that should accompany the reporting of these results. In particular, when Lasso/L1 regularization algorithms encounter 2 predictors that

are strongly correlated, they will tend to select one and eliminate the other, rather than jointly shrinking the 2 coefficients and keeping both (as in Ridge/L2 regression; Tibshirani 1996; Ng 2004). This process enforces sparsity and simplicity in the resultant model, but theoretically, may not consistently select the same predictors each time it is run on the same input data. Accordingly, it may be less reliable in identifying specific features out of a group of highly correlated features (i.e., within-network voxels) that differ between 22q11DS patients and controls. However, the notable performance of the ACC/precuneus, DMN, and posterior DMN-derived classifiers in the independent Syracuse cohort provides strong evidence for the generalizability of the observed connectivity deficits within these networks.

Aside from the technical considerations raised above, some additional limitations should be noted. First, in addition to the unequivocal association of 22q11DS with psychosis, other psychiatric comorbidities (e.g., ADHD, ASD, and anxiety) are commonly observed in patients with 22q11DS (Schneider et al. 2014) and could present a potential confound for observed group differences. However, our follow-up sensitivity analyses revealed that none of the ICN-derived classifiers that distinguished 22q11DS patients at high versus low risk for psychosis were able to distinguish between 22q11DS subjects with or without an ADHD diagnosis, nor those with or without ASD, suggesting that the connectivity deficits encoded by these classifiers are specific to psychosis risk. Patients in the 22qHR and 22qLR groups also did not differ in IQ or other demographic factors in either cohort, indicating that the accurate HR versus LR classification was not attributable to general cognitive or other differences between groups. Second, the cross-sectional nature of the study is a limitation. Data from individuals at clinical HR for psychosis (defined by high SIPS scores) indicate an ~35% rate of conversion to overt psychotic disorder within 3 years following ascertainment (Cannon et al. 2008; Fusar-Poli et al. 2012). Using similar HR criteria, Klosterkötter et al. (2001) found that 79/160 (49%) of individuals with prodromal symptoms developed a psychotic disorder over a 9.6-year period. While elevated SIPS positive symptoms are consistently associated with risk for conversion to overt psychosis (Cannon et al. 2008; Perkins et al. 2015), we do not know what portion of HR 22q11DS subjects will ultimately develop overt psychosis. Thus, longitudinal validation of the psychosis-risk ICN signatures for predicting the development of an overt psychotic disorder is an important next step. Third, given that some studies suggest that motion may increase local connectivity while reducing BOLD signal correlations between distant areas (Power et al. 2012; Van Dijk et al. 2012; Satterthwaite et al. 2013), it is important to consider the possibility that differential motion between 22q11DS cases and controls could have contributed to our findings of hypoconnectivity in 22q11DS. In the present study, ICA was used to identify and remove motion-related noise signal. It is possible that some noise-related signal persisted in our data. However, given that 22q11DS and control subjects showed similar amounts of motion at each site, and that similar patterns of hypoconnectivity were found across ICNs when group comparisons were restricted to subgroups of subjects with minimal motion, it is unlikely that differences in connectivity could be accounted for by differential motion effects. Finally, it should be noted that while the diagnostic classification accuracy of the ACC/precuneus, DMN and posterior DMN-derived classifiers was high in both the UCLA training- and Syracuse testing-cohorts, the average accuracy of these classifiers was lower in the test cohort (i.e., 73%). Similarly, the average accuracy of the ACC/precuneus, DMN, left executive, and salience-derived classifiers for distinguishing 22q11DS youth at high versus low risk for psychosis was lower in the test cohort (81.5%) relative to the training cohort (89.25%). Further work is therefore needed before these classifiers are appropriate for clinical use.

The findings presented in this work highlight the within-network connectivity deficits that appear to be a hallmark of 22q11DS throughout the critical period of adolescence and into early adulthood, when individuals are most at risk of developing a psychotic disorder. Classifiers derived from the ACC/precuneus network, the DMN, and the posterior DMN were the most robust, highlighting the marked reduction of long-range communication in networks anchored along the cortical midline in adolescents with 22q11DS. These 3 classifiers generalized to an independent sample of young adults, suggesting that ICN hypoconnectivity within these networks may be a stable distinguishing feature of 22q11DS over time. Finally, the robust and predictable variation in ICN-coherence (within the ACC/precuneus, DMN, left executive, and salience networks) between the $22q_{HR}$ and $22q_{LR}$ groups allows the reliable identification of 22q11DS subjects at HR of developing a psychotic disorder. These findings suggest a replicable biomarker that may aid in the identification of a nascent psychiatric disorder.

Supplementary Material

Supplementary material are available at *Cerebral Cortex* online.

Funding

National Institute of Mental Health and National Institute on Aging at the National Institutes of Health (F31 MH099786 to M.J.S.; T32 MH096682 to J.K.F.; R03 MH106922 to A.E.A.; K25 AG051782 to A.E.A.; RO1 MH064824 to W.R.K.; and RO1 MH80953 to C.E.B.) and the Achievement Rewards For College Scientists (ARCS) Foundation (ARCS Fellowship to M.J.S.). A.E.A. holds a Career Award at the Scientific Interface from BWF.

Notes

The authors gratefully acknowledge the sources of support mentioned above, and have no conflicts of interest to report. Address correspondence to Carrie E. Bearden, A7-460 Semel Institute, Los Angeles, CA 90095, USA. E-mail: cbearden@mednet.ucla.edu.

References

Addington J, Cadenhead KS, Cornblatt BA, Mathalon DH, McGlashan TH, Perkins DO, Seidman LJ, Tsuang MT, Walker EF, Woods SW, et al. 2012. North American prodrome longitudinal study (NAPLS 2): overview and recruitment. Schizophr Res. 142(1):77–82.

Alderson-Day B, McCarthy-Jones S, Fernyhough C. 2015. Hearing voices in the resting brain: a review of intrinsic functional connectivity research on auditory verbal hallucinations. Neurosci Biobehav Rev. 55:78–87.

Alonso-Solís A, Vives-Gilabert Y, Grasa E, Portella MJ, Rabella M, Sauras RB, Roldán A, Núñez-Marín F, Gómez-Ansón B, Pérez V, et al. 2015. Resting-state functional connectivity alterations in the default network of schizophrenia patients with persistent auditory verbal hallucinations. Schizophr Res. 161(2–3):261–268.

Anticevic A, Cole MW, Repovs G, Murray JD, Brumbaugh MS, Winkler AM, Savic A, Krystal JH, Pearlson GD, Glahn DC. 2014. Characterizing thalamo-cortical disturbances in

schizophrenia and bipolar illness. Cereb Cortex. 24(12): 3116–3130.

Antshel KM, Shprintzen R, Fremont W, Higgins AM, Faraone SV, Kates WR. 2010. Cognitive and psychiatric predictors to psychosis in velocardiofacial syndrome: a 3-year follow-up study. J Am Acad Child Adolesc Psychiatry. 49(4):333–344.

Bearden CE, van Erp TG, Dutton RA, Tran H, Zimmermann L, Sun D, Geaga JA, Simon TJ, Glahn DC, Cannon TD, et al. 2007. Mapping cortical thickness in children with 22q11.2 deletions. Cereb Cortex. 17(8):1889–1898.

Beckmann CF, Smith SM. 2004. Probabilistic independent component analysis for functional magnetic resonance imaging. IEEE Trans Med Imaging. 23(2):137–152.

Beckmann CF. 2009. Group comparison of resting-state FMRI data using multi-subject ICA and dual regression. OHBM. https://pdfs.semanticscholar.org/25fd/7d29fc3c1b2fd07fb0d4390ded585ede3978.pdf.

Biswal B, Yetkin FZ, Haughton VM, Hyde JS. 1995. Functional connectivity in the motor cortex of resting human brain using echo-planar MRI. Magn Reson Med. 34(4):537–541.

Broyd SJ, Demanuele C, Debener S, Helps SK, James CJ, Sonuga-Barke EJ. 2009. Default-mode brain dysfunction in mental disorders: a systematic review. Neurosci Biobehav Rev. 33(3): 279–296.

Calhoun VD, Liu J, Adali T. 2009. A review of group ICA for fMRI data and ICA for joint inference of imaging, genetic, and ERP data. Neuroimage. 45:163–172.

Calhoun VD, Sui J, Kiehl K, Turner J, Allen E, Pearlson G. 2012. Exploring the psychosis functional connectome: aberrant intrinsic networks in schizophrenia and bipolar disorder. Front Psychiatry. 2(75):1–13.

Cannon TD, Cadenhead K, Cornblatt B, Woods SW, Addington J, Walker E, Seidman LJ, Perkins D, Tsuang M, McGlashan T, et al. 2008. Prediction of psychosis in youth at high clinical risk: a multisite longitudinal study in North America. Arch Gen Psychiatry. 65(1):28–37.

Chun S, Westmoreland JJ, Bayazitov IT, Eddins D, Pani AK, Smeyne RJ, Yu J, Blundon JA, Zakharenko SS. 2014. Specific disruption of thalamic inputs to the auditory cortex in schizophrenia models. Science. 344(6188):1178–1182.

Coman IL, Gnirke MH, Middleton FA, Antshel KM, Fremont W, Higgins AM, Shprintzen RJ, Kates WR. 2010. The effects of gender and catechol O-methyltransferase (COMT) $Val^{108/158}$Met polymorphism on emotion regulation in velo-cardio-facial syndrome (22q11.2 deletion syndrome): an fMRI study. Neuroimage. 53(3):1043–1050.

Debbane M, Lazouret M, Lagioia A, Schneider M, Van De Ville D, Eliez S. 2012. Resting-state networks in adolescents with 22q11.2 deletion syndrome: associations with prodromal symptoms and executive functions. Schizophr Res. 139: 33–39.

Drew LJ, Crabtree GW, Markx S, Stark KL, Chaverneff F, Xu B, Mukai J, Fenelon K, Hsu PK, Gogos JA, et al. 2011. The 22q11.2 microdeletion: fifteen years of insights into the genetic and neural complexity of psychiatric disorders. Int J Dev Neurosci. 29(3):259–281.

First MB, Spitzer RL, Gibbon M, Williams JBW. 1996. Structured Clinical Interview for DSM-IV Axis I Disorders, Clinician Version (SCID-CV). Washington, DC: American Psychiatric Press, Inc.

Fusar-Poli P, Bonoldi I, Yung AR, Borgwardt S, Kempton MJ, Valmaggia L, Barale F, Caverzasi E, McGuire P. 2012. Predicting psychosis: meta-analysis of transition outcomes in individuals at high clinical risk. Arch Gen Psychiatry. 69(3):220–229.

Griffanti L, Salimi-Khorshidi G, Beckmann CF, Auerbach EJ, Douaud G, Sexton CE, Zsoldos E, Ebmeier KP, Filippini N, Mackay CE, et al. 2014. ICA-based artefact removal and accelerated fMRI acquisition for improved resting state network imaging. NeuroImage. 95:232–247.

Ho JS, Radoeva PD, Jalbrzikowski M, Chow C, Hopkins J, Tran WC, Mehta A, Enrique N, Gilbert C, Antshel KM, et al. 2012. Deficits in mental state attributions in individuals with 22q11. 2 deletion syndrome (velo-cardio-facial syndrome). Autism Res. 5(6):407–418.

Jalbrzikowski M, Carter C, Senturk D, Chow C, Hopkins JM, Green MF, Galván A, Cannon TD, Bearden CE. 2012. Social cognition in 22q11.2 microdeletion syndrome: relevance to psychosis. Schizophr Res. 142(1-3):99–107.

Jenkinson M, Bannister PR, Brady JM, Smith SM. 2002. Improved optimisation for the robust and accurate linear registration and motion correction of brain images. NeuroImage. 17(2): 825–841.

Kates WR, Antshel KM, Faraone SV, Fremont WP, Higgins AM, Shprintzen RJ, Botti JA, Kelchner L, McCarthy C. 2011. Neuroanatomic predictors to prodromal psychosis in velocardiofacial syndrome (22q11.2 deletion syndrome): a longitudinal study. Biol Psychiatry. 69(10):945–952.

Kelly RE, Alexopoulos GS, Wang Z, Gunning FM, Murphy CF, Morimoto SS, Kanellopoulos D, Jia Z, Lim KO, Hoptman MJ. 2010. Visual inspection of independent components: defining a procedure for artifact removal from fMRI data. J Neurosci Methods. 189(2):233–245.

Klosterkötter J, Hellmich M, Steinmeyer EM, Schultze-Lutter F. 2001. Diagnosing schizophrenia in the initial prodromal phase. Arch Gen Psychiatry. 58(2):158–164.

Littow H, Huossa V, Karjalainen S, Jääskeläinen E, Haapea M, Miettunen J, Tervonen O, Isohanni M, Nikkinen J, Veijola J, et al. 2015. Aberrant functional connectivity in the default mode and central executive networks in subjects with schizophrenia—a whole-brain resting-state ICA study. Front Psychiatry. 6(26):1–10.

Mattiaccio LM, Coman IL, Schreiner MJ, Antshel KM, Fremont WP, Bearden CE, Kates WR. 2016. Atypical functional connectivity in resting networks of individuals with 22q11.2 deletion syndrome: associations with neurocognitive and psychiatric functioning. J Neurodev Disorder. 8:2.

McCarthy CS, Ramprashad A, Thompson C, Botti JA, Coman IL, Kates WR. 2015. A comparison of FreeSurfer-generated data with and without manual intervention. Front Neurosci. 9:379.

Meechan DW, Tucker ES, Maynard TM, LaMantia AS. 2009. Diminished dosage of 22q11 genes disrupts neurogenesis and cortical development in a mouse model of 22q11 deletion/DiGeorge syndrome. PNAS USA. 106(38):16434–16445.

Meechan DW, Maynard TM, Tucker ES, Fernandez A, Karpinski BA, Rothblat LA, LaMantia AS. 2015. Modeling a model: mouse genetics, 22q11.2 deletion syndrome, and disorders of cortical circuit development. Prog Neurobiol. 130:1–28.

Menon V. 2011. Large-scale brain networks and psychopathology: a unifying triple network model. Trends Cogn Sci. 15(10): 483–506.

Miller TJ, McGlashan TH, Rosen JL, Cadenhead K, Cannon T, Ventura J, McFarlane W, Perkins DO, Pearlson GD, Woods SW. 2003. Prodromal assessment with the structured interview for prodromal syndromes and the scale of prodromal symptoms:

predictive validity, interrater reliability, and training to reliability. Schizophr Bull. 29(4):703–715.

Monks S, Niarchou M, Davies AR, Walters JT, Williams N, Owen MJ, van den Bree MB, Murphy KC. 2014. Further evidence for high rates of schizophrenia in 22q11.2 deletion syndrome. Schizophr Res. 153(1–3):231–236.

Mohr H, Wolfensteller U, Frimmel S, Ruge H. 2015. Sparse regularization techniques provide novel insights into outcome integration processes. NeuroImage. 104:163–176.

Murphy KC. 2002. Schizophrenia and velo-cardio-facial syndrome. Lancet. 359(9304):426–430.

Ng A 2004. Feature selection, L1 vs. L2 regularization, and rotational invariance. Proceedings of the 21st International Conference on Machine Learning.

Ottet MC, Schaer M, Debbané M, Cammoun L, Thiran JP, Eliez S. 2013. Graph theory reveals dysconnected hubs in 22q11DS and altered nodal efficiency in patients with hallucinations. Front Hum Neurosci. 7(402):1–10.

Pereira F, Mitchell T, Botvinick M. 2009. Machine learning classifiers and fMRI: a tutorial overview. Neuroimage. 45:199–209.

Perkins DO, Jeffries CD, Cornblatt BA, Woods SW, Addington J, Bearden CE, Cadenhead KS, Cannon TD, Heinssen R, Mathalon DH, et al. 2015. Severity of thought disorder predicts psychosis in persons at clinical high-risk. Schizophr Res. 169(1–3):169–177.

Plitt M, Barnes KA, Wallace GL, Kenworthy L, Martin A. 2015. Resting-state functional connectivity predicts longitudinal change in autistic traits and adaptive functioning in autism. PNAS USA. 112(48):E6699–E6706.

Power JD, Barnes KA, Snyder AZ, Schlaggar BL, Petersen SE. 2012. Spurious but systematic correlations in functional connectivity MRI networks arise from subject motion. Neuroimage. 59(3):2142–2154.

Rizk-Jackson A, Stoffers D, Sheldon S, Kuperman J, Dale A, Goldstein J, Corey-Bloom J, Poldrack RA, Aron AR. 2011. Evaluating imaging biomarkers for neurodegeneration in pre-symptomatic Huntington's disease using machine learning techniques. Neuroimage. 56(2):788–796.

Roizen NJ, Higgins AM, Antshel KM, Fremont W, Shprintzen R, Kates WR. 2010. 22q11.2 deletion syndrome: are motor deficits more than expected for IQ level? J Pediatr. 157(4):658–661.

Rosa MJ, Portugal L, Hahn T, Fallgatter AJ, Garrido MI, Shawe-Taylor J, Mourao-Miranda J. 2015. Sparse network-based models for patient classification using fMRI. Neuroimage. 105:493–506.

Ryali S, Supekar K, Abrams DA, Menon V. 2010. Sparse logistic regression for whole-brain classification of fMRI data. NeuroImage. 51(2):752–764.

Satterthwaite TD, Elliott MA, Gerraty RT, Ruparel K, Loughead J, Calkins ME, Eickhoff SB, Hakonarson H, Gur RC, Gur RE, et al. 2013. An improved framework for confound regression and filtering for control of motion artifact in the preprocessing of resting-state functional connectivity data. Neuroimage. 64: 240–256.

Scariati E, Schaer M, Richiardi J, Schneider M, Debbané M, Van De Ville D, Eliez S. 2014. Identifying 22q11.2 deletion syndrome and psychosis using resting-state connectivity patterns. Brain Topogr. 6:808–821.

Schneider M, Debbané M, Bassett AS, Chow EW, Fung WL, van den Bree M, Owen M, Murphy KC, Niarchou M, Kates WR, et al, International Consortium on Brain and Behavior in 22q11.2 Deletion Syndrome. 2014. Psychiatric disorders from childhood to adulthood in 22q11.2 deletion syndrome: results from the International Consortium on Brain and Behavior in 22q11.2 Deletion Syndrome. Am J Psychiatry. 171(6):627–639.

Schreiner M, Lazaro MT, Jalbrzikowski M, Bearden CE. 2013. Converging levels of analysis on a genomic hotspot for psychosis: insights from 22q11.2 deletion syndrome. Neuropharmacology. 68:157–173.

Schreiner M, Karlsgodt KH, Uddin LQ, Chow C, Congdon E, Jalbrzikowski M, Bearden CE. 2014. Default mode network connectivity and reciprocal social behavior in 22q11.2 deletion syndrome. SCAN. 9(9):1261–1267.

Shaffer D, Fisher P, Dulcan MK, Davies M, Piacentini J, Schwab-Stone ME, Lahey BB, Bourdon K, Jensen PS, Bird HR, et al. 1996. The NIMH diagnostic interview schedule for children version 2.3 (DISC-2.3): description, acceptability, prevalence rates, and performance in the MECA study. J Am Acad Child Adolesc Psychiatry. 35(7):865–877.

Shaikh TH, Kurahashi H, Saitta SC, O'Hare AM, Hu P, Roe BA, Driscoll DA, McDonald-McGinn DM, Zackai EH, Budarf ML, et al. 2000. Chromosome 22-specific low copy repeats and the 22q11.2 deletion syndrome: genomic organization and deletion endpoint analysis. Hum Mol Genet. 9(4):489–501.

Shashi V, Francis A, Hooper SR, Kranz PG, Zapadka M, Schoch K, Ip E, Tandon N, Howard TD, Keshavan MS. 2012. Increased corpus callosum volume in children with chromosome 22q11.2 deletion syndrome is associated with neurocognitive deficits and genetic polymorphisms. Eur J Hum Genet. 20(10): 1051–1057.

Tibshirani R. 1996. Regression shrinkage and selection via the Lasso. J R Stat Soc B. 58:267–288.

Thomason ME, Dennis EL, Joshi AA, Joshi SH, Dinov ID, Chang C, Henry ML, Johnson RF, Thompson PM, Toga AW, et al. 2011. Resting-state fMRI can reliably map neural networks in children. Neuroimage. 55(1):165–175.

Uddin LQ, Supekar K, Lynch CJ, Khouzam A, Phillips J, Feinstein C, Ryali S, Menon V. 2013. Salience network-based classification and prediction of symptom severity in children with autism. JAMA Psychiatry. 70(8):869–879.

Van Dijk KR, Sabuncu MR, Buckner RL. 2012. The influence of head motion on intrinsic functional connectivity MRI. Neuroimage. 59(1):431–438.

Varoquaux G, Raamana PR, Engemann DA, Hoyos-Idrobo A, Schwartz Y, Thirion B. 2017. Assessing and tuning brain decoders: cross-validation, caveats, and guidelines. NeuroImage. 145:166–179.

Van den Heuvel MP, Hulshoff Pol HE. 2010. Exploring the brain network: a review on resting-state fMRI functional connectivity. Eur Neuropsychopharmacol. 20(8):519–534.

Vega JN, Hohman TJ, Pryweller JR, Dykens EM, Thornton-Wells TA. 2015. Resting-state functional connectivity in individuals with Down syndrome and Williams syndrome compared with typically developing controls. Br Connect. 5(8): 461–475.